Study on a Hybrid Superconducting Magnetic Bearing System

Fang J., Lin L., and Yan L.

Institute of Electrical Engineering, Chinese Academy of Sciences Beijing, 100080, China

High temperature superconducting magnetic bearings have several significant advantages over conventional magnetic bearings. However, the low stiffness, low damping, and the uncertainty of working displacement make it impracticable to realize a superconducting magnetic bearing. In order to deal with these problems, a hybrid superconducting magnetic bearing system which consists of superconducting magnetic bearings, permanent magnetic bearings, and active magnetic bearings has been developed. In this paper, the five-degree motion equation of the rotor has been built, and the distributed control method is used to control active magnetic bearings. The experimental results of the small hybrid superconducting magnetic bearing system are presented.

INTRODUCTION

One of the practical applications of high temperature superconductors (HTS) is the superconducting magnetic bearing (SMB) [1]. In comparison with the active magnetic bearings (AMB), however, the SMB has two main problems: one is low stiffness and damping because of no feedback control system, and another is the initial loading equipment due to magnetic flux creep or flux flow, and the differences of levitation forces between zero-field cooling (ZFC) and field cooling (FC).

In order to resolve the above problems, we have designed and constructed a small experimental flywheel system which consists of three kinds of magnetic bearings: SMB, AMB, and permanent magnetic bearings (PMB).

In this paper, the five-degree motion equation of the rotor is discussed by using force analyses and rotor dynamics. The distributed control method is used to control active magnetic bearings and some experimental results of the small hybrid superconducting magnetic bearing system are presented.

STRUCTURE

We designed and built a small hybrid SMB experimental device. The schematic illustration of hybrid SMB is shown in Figure 1. In this system, an axial PMB is located at the top of the rotor; two radial AMBs are added in the radial directions; a SMB is located at the bottom of the rotor. The design specifications of three kinds of magnetic bearings were reported in [2], and the numerical and experimental analyses of SMB and PMB were presented in [3]. In this design, the axial PMB is applied to levitate the weight of the rotor, and initially position the rotor in the axial direction. In addition, two radial AMBs are applied to improve the magnitude of radial stiffness and damping of the rotor and initially position the rotor in the radial direction.

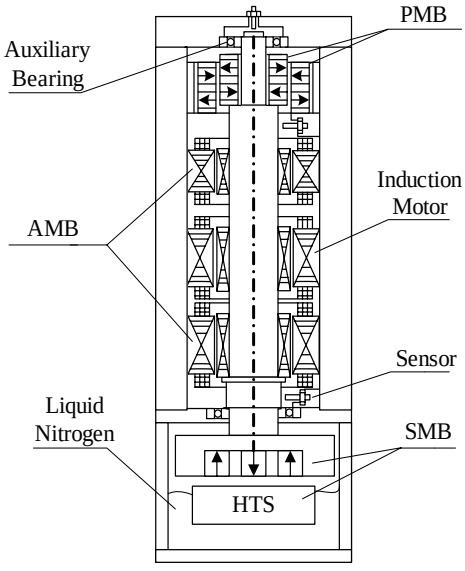

Figure 1 Schematic illustration of hybrid SMB

ANALYSES OF FORCES

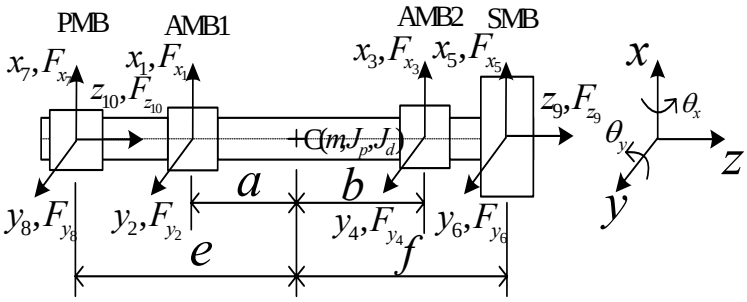

Figure 2 The rotor model

As shown in Figure 2, the rotor receives totally ten forces from magnetic bearings with exception of gravity along the axial degree z. F_{x1}, F_{y2}, F_{x3}, and F_{y4} are the forces acting on the rotor along the four radial degrees x_1, y_2, x_3, and y_4 by two AMBs: AMB1 and AMB2. F_{x5}, F_{y6}, and F_{z9} are the forces acting on the rotor along the two radial degrees x_5, y_6, and the axial degree z_9 by SMB. F_{x7}, F_{y8}, and F_{z10} are the forces along the two radial degrees x_7, y_8, and the axial degree z_{10} by PMB.

SMB can obtain intrinsic stability in all three directions due to the Meissner effect and flux pinning center. With the axial PMB, the hybrid system can suspend the rotor in FC condition. For SMB and PMB, the interaction forces between superconductors and permanent magnets along the three degrees x_5, y_6, and z_9, and the interaction forces between the stator and rotor permanent magnets along the three degrees x_7, y_8, and z_{10} can be linearized around their nominal equilibrium operation points by

$$\begin{cases} F_{x5} = -k_{x5} \cdot x_5 \\ F_{y6} = -k_{y6} \cdot y_6 \\ F_{z9} = -k_{z9} \cdot z_9 \\ F_{x7} = -k_{x7} \cdot x_7 \\ F_{y8} = -k_{y8} \cdot y_8 \\ F_{z10} = -k_{z10} \cdot z_{10} - mg \end{cases} \tag{1}$$

where m is the mass of the rotor; $k_{x5}, k_{y6},$ and k_{z9} are SMB stiffness constants; and k_{x7}, k_{y8}, and k_{z10} are PMB stiffness constants.

For AMB, the nonlinear current-force dependence is linearized by supplying a bias current into both coils at opposite sides of the rotor. Neglecting the coupling of sensor locations and magnetic circuits, the forces of two radial AMBs along the four radial degrees x_1, y_2, x_3, and y_4 can be linearized by

$$\begin{cases} F_{xj} = k_{cj} \cdot i_{cj} + k_{dj} \cdot x_j \\ F_{yj} = k_{cj} \cdot i_{cj} + k_{dj} \cdot y_j \end{cases} \tag{2}$$

where $j = 1,2,3,4$ refer to the four radial degrees x_1, y_2, x_3, y_4, k_d is the force-displacement coefficient, and k_c is the force-current coefficient.

SYSTEM MODEL

Assuming that the rotor is rigid and the coordinate for the rotor is set as shown in Figure 2, the dynamic five-degree motion equations for the rotor of the hybrid superconducting magnetic bearing system are

$$\begin{cases} m\ddot{x} = F_{x1} + F_{x3} + F_{x5} + F_{x7} \\ m\ddot{y} = F_{y2} + F_{y4} + F_{y6} + F_{y8} \\ J_d\ddot{\theta}_x + J_p\dot{\theta}_y\omega = aF_{y2} + eF_{y8} - bF_{y4} - fF_{y6} \\ J_d\ddot{\theta}_y - J_p\dot{\theta}_x\omega = -aF_{x1} - eF_{x7} + bF_{x3} + fF_{x5} \\ m\ddot{z} = F_{z9} + F_{z10} + mg \end{cases} \tag{3}$$

where J_d is the transversal inertia moment, J_p is the polar inertia moment, ω is the angular velocity of the mass center, θ_x and θ_y are rotation angles for the rotor, and a, b, e, and f are distances between the center of upper AMB1, lower AMB2, PMB, SMB and the mass center, respectively.

After linearizations of all three kinds of magnetic bearings, substituting (1-2) and the transfer equations from the coordinate $(x, y, \theta_x, \theta_y)$ and (x_5, y_6, x_7, y_8) to (x_1, y_2, x_3, y_4) into (3), we can obtain the motion equations of the rotor based on the coordinate (x_1, y_2, x_3, y_4, z), and design the controller of AMB to get the desirable higher stiffness than that of SMB and PMB by nearly two orders of magnitude [2-3]. Therefore, the stiffness of the hybrid system will be mainly dependent on the stiffness of AMB in the four radial degrees x_1, y_2, x_3, and y_4. According to the principle of the rotor dynamics, the motion along the axial degree z is independent of the motions along the radial degrees. In (3), neglecting F_{x5} and F_{y6} acting on SMB, and F_{x7} and F_{y8} acting on PMB, with the transfer equations from the coordinate $(x, y, \theta_x, \theta_y)$ to (x_1, y_2, x_3, y_4), we can obtain the motion equations of the rotor in the four radial degrees x_1, y_2, x_3, y_4. Assuming that the state vector, the control vector, and output vector are $X(t) = [x_1, x_3, y_2, y_4, \dot{x}_1, \dot{x}_3, \dot{y}_2, \dot{y}_4]^{\mathrm{T}}$, $U(t) = [i_1, i_3, i_2, i_4]^{\mathrm{T}}$, and $Y(t) = [x_1, x_3, y_2, y_4]^{\mathrm{T}}$, respectively, the state space model is presented as

$$\begin{cases} \dot{X}(t) = A(t)X(t) + B(t)U(t) \\ Y(t) = CX(t) \end{cases} \tag{4}$$

where $A(t) = \begin{bmatrix} 0 & 0 & I_2 & 0 \\ 0 & 0 & 0 & I_2 \\ K_{13} & 0 & 0 & -G \\ 0 & K_{24} & G & 0 \end{bmatrix}$, $B(t) = \begin{bmatrix} 0 & 0 \\ 0 & 0 \\ H_{13} & 0 \\ 0 & H_{24} \end{bmatrix}$, $C = [I_4 \quad 0]$,

where $G = \dfrac{\omega \cdot J_p}{l \cdot J_d} \begin{bmatrix} a & -a \\ -b & b \end{bmatrix}$, $K_{ij} = \dfrac{1}{m} \begin{bmatrix} k_{di}\left(1 + \dfrac{a^2}{\rho^2}\right) & k_{dj}\left(1 - \dfrac{ab}{\rho^2}\right) \\ k_{di}\left(1 - \dfrac{ab}{\rho^2}\right) & k_{dj}\left(1 + \dfrac{b^2}{\rho^2}\right) \end{bmatrix}$, $H_{ij} = \dfrac{1}{m} \begin{bmatrix} k_{ci}\left(1 + \dfrac{a^2}{\rho^2}\right) & k_{cj}\left(1 - \dfrac{ab}{\rho^2}\right) \\ k_{ci}\left(1 - \dfrac{ab}{\rho^2}\right) & k_{cj}\left(1 + \dfrac{b^2}{\rho^2}\right) \end{bmatrix}$,

where $i = 1,2$, $j = 3,4$ and $\rho^2 = \dfrac{J_d}{m}$.

CONTROL DESIGN

Through the structure design, some mechanical couplings in (4) can be reduced to a large extent to be negligible, and motions of the rotor along the four radial degrees can be decoupled. At low speeds, neglecting the gyroscopic effect G, the transfer function of AMB $W_o(s)$ in every degree relating the state output to control can be simplified as

$$W_o(s) = \frac{X(s)}{U(s)} = \frac{k_c}{m_i s^2 - k_d} \tag{5}$$

where $m_i = m\dfrac{\rho^2}{\rho^2 + i^2}$, and $i = a, b$.

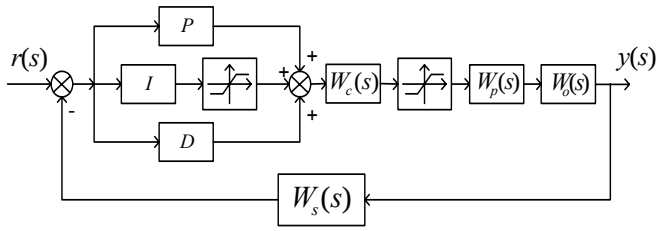

Figure 3 Block diagram of nonlinear control system

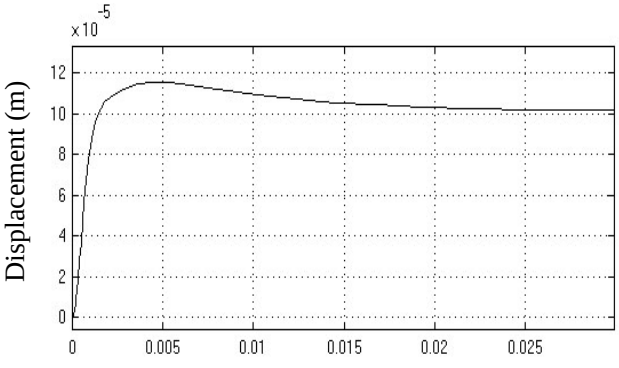

Figure 4 The step response of nonlinear control system

The characteristics of the stiffness and damping of AMB mainly depend on the electrical control system, and the controller can be designed as the desired stiffness and damping. Figure 3 shows the block diagram of the applied nonlinear control system, where $W_c(s)$, $W_p(s)$, $W_o(s)$, and $W_s(s)$ are transfer functions of the phase-lead compensator, power amplifier, plant, and sensor, respectively. The integrator (I) is added into the PD controller in order to reduce the steady errors. Two nonlinear saturation components are joined to limit the effect of the integrator and simulate the saturation of electromagnets. The phase-lead compensator is applied to improve the stability of control system. The unit step response simulation of the nonlinear control system is shown in Figure 4. The overshoot of the step response is about 15%, and the settling time is about 20ms.

EXPERIMENTAL RESULTS

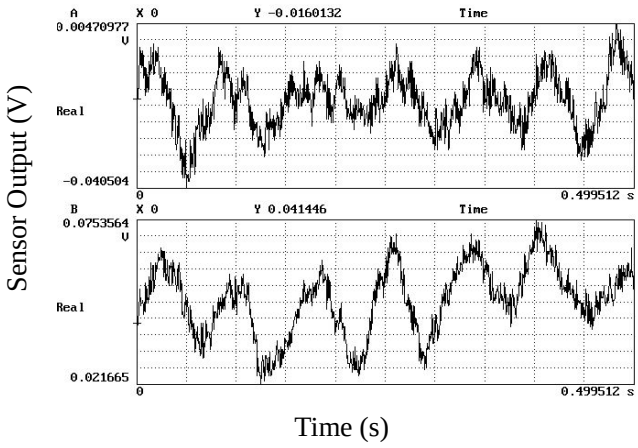

Figure 5 Vibration characteristics of the rotor along x_3 and y_4 at steady state

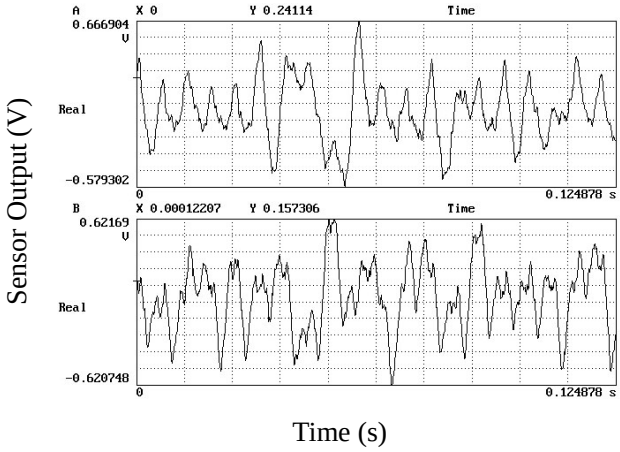

Figure 6 Vibration characteristics of the rotor along x_3 and y_4 at speeds of 9,600 rpm

Using above nonlinear controller, the 3.5 kg rotor of the hybrid superconducting magnetic system has been levitated by PMB and SMB in axial direction, and can be accelerated with the assistance of AMB in radial directions. The vibration characteristics of the rotor along the degree x_3 and y_4 at steady state is shown in Figure 5. The transfer function of the sensor is 20mV/μm, so the rotor vibration is within 5 μm at steady state. Figure 6 shows the vibration of the rotor along the two degrees x_3 and y_4 at speeds of 9,600 rpm with vibration amplitude of about 30 μm.

CONCLUSION

In this paper, the five-degree motion equation of the rotor has been built by means of the linearization of the forces of three kinds of magnetic bearings, and rotor dynamics. The stiffness of the hybrid system is mainly dependent on the stiffness of active magnetic bearings in the four radial degrees, and the distributed control method is used to control active magnetic bearings. Using a nonlinear controller with phase-lead compensator, the rotor vibration along the degree x_3 and y_4 is within a 5 μm at steady state, and about 30 μm vibration amplitude at speeds of 9,600 rpm. The experimental results show that the hybrid superconducting magnetic bearing system is effective in the view of the distributed control system.

REFERENCES

1. Moon, F., Superconducting Levitation, 1st edition, John Willey & Sons, Inc., New York, USA (1993)
2. Fang, J., Lin, L., Yan, L. and Xiao, L., A new flywheel energy storage system using hybrid superconducting magnetic bearings, *IEEE Trans. on Appl. Supercon* (2001) Vol. 11, No. 1, 1657-1660
3. Fang, J., Lin, L. and Yan, L., Numerical analysis of a new hybrid superconducting magnetic bearing flywheel system, Advances in Cryogenic Engineering, Proceeding of CEC (2002) 47, 465-472